Response to reviewer 1's comments for Operational performance of the Vaisala CL61 ceilometer for atmospheric profiling

Viet Le[1], Ewan J. O'Connor[1], Maria Filioglou[2], and Ville Vakkari[1, 3]

[1]Finnish Meteorological Institute, Helsinki, 00101, Finland
[2]Finnish Meteorological Institute, Atmospheric Research Centre of Eastern Finland, Kuopio, Finland
[3]Atmospheric Chemistry Research Group, Chemical Resource Beneficiation, North-West University, Potchefstroom, 2520, South Africa

Correspondence: viet.le@fmi.fi

We would like to thank the reviewers for the constructive comments. Below are the reviewer comments in black text, followed by our responses in blue text. Where applicable, we also provide changes to the manuscript in *blue italics*.

1 General comments

The study by Le et al. focuses on evaluating several instrumental characteristics of the Vaisala CL61 ceilometer for aerosol vertical profiling applications. The manuscript addresses the quantification of instrumental artifacts in the measurements, in terms of bias and noise, based on several years of observations acquired both with and without a termination hood, and proposes methods to correct for these instrumental effects. In addition, the authors describe an automated calibration methodology based on liquid cloud layers and highlight signal drifts that are attributed to instrumental effects.

Overall, the manuscript is well written and allows the reader to follow most of the methodological steps taken by the authors. The topic is of considerable interest to the atmospheric remote sensing community, as this instrument - commercially available in recent years - is becoming increasingly widespread. I therefore recommend publication of the manuscript after addressing the minor comments listed below.

We would like to thank the reviewer for their positive evaluation of the manuscript.

2 Specific comments

The study refers to the difference between the background signal during daytime and nighttime conditions (e.g., Section 4.1 and Fig. 5). However, it is not entirely clear whether this difference is actually exploited to quantitatively validate the results obtained with more accurate measurements (e.g., those acquired with the termination hood). For sites or networks where the termination hood is not available, could nighttime measurements under pristine conditions be considered a reasonable proxy for estimating instrumental noise (without solar background)?

The following has been added to Sect. 3.1

In principle, the nighttime measurements could be used to estimate $P_{\text{instrument}}$. However, only the portion of the $P_{\text{instrument}}$ profile at higher ranges, where clouds and aerosols are absent, can be reliably estimated. An example is shown in Fig. S2 in the Supplement, where σ^2_{ppol/r^2} agrees well between the hood termination and nighttime measurements only at ranges above approximately 2 km. This agreement is observed only under clear-sky conditions, as cloud layers at lower ranges can increase the measured values.

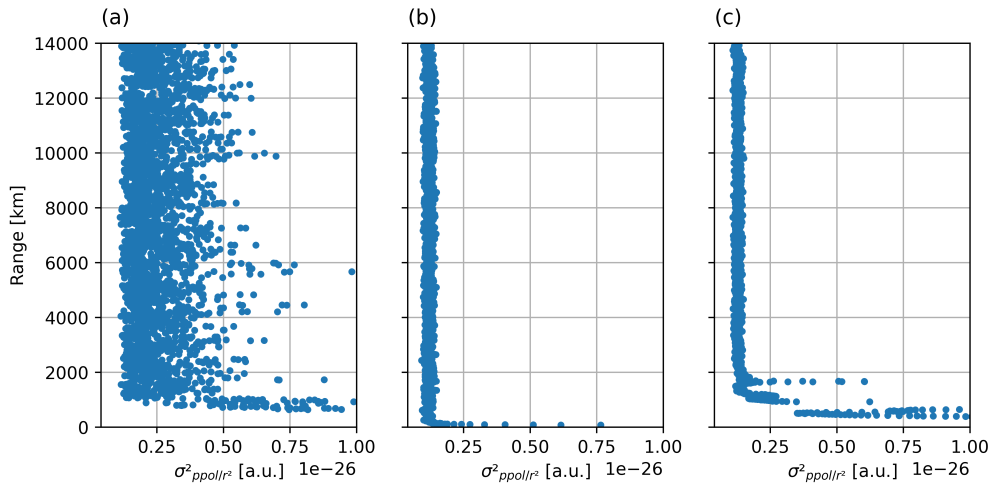

Figure S2. *Example of σ^2_{ppol/r^2} profile in Kenttärova during a) a cloudy night on 2024-03-05 00:00 to 02:00 UTC, b) termination hood measurement on 2024-03-05 14:00 to 15:00 UTC, c) a clear-sky night on 2024-03-06 20:00 to 22:00 UTC.*

Firmware corrections: it may be useful to provide additional details—within the limits of the manufacturer's documentation—on how the firmware attempts to compensate for both the background signal and sensitivity variations (i.e., calibration coefficient). For instance, is a test LED used for internal monitoring of sensitivity changes? How is the firmware compensation handled during measurements performed with the termination hood?

To our knowledge, no test LED is included in the setup. For the termination hood measurement, no information is passed on to the instrument hardware, so the measurements are continued exactly as during usual atmospheric observations. This is why the termination hood can be used to quantify instrumental performance and bias in the near range.

The following are included in the text regarding the firmware:

...and C_L represents the lidar constant. This constant encapsulates the system-specific characteristics of the lidar, such as its receiver optics and laser properties. It is initially determined and provided by the manufacturer, but it may drift over time as the instrument ages and its performance changes. Although the internal firmware attempts to monitor and compensate for these changes, additional calibration, such as absolute calibration using stratocumulus clouds, is still necessary...

...The hood was applied without modifying the instrument's internal operating parameters, ensuring that all measurements reflected normal operational conditions...

σ_R: the approximation introduced at line 245 and in Eq. (31) appears to be dimensionally inconsistent. β_p is expressed in m^{-1} sr^{-1}, whereas R is defined as a ratio between two backscatter coefficients. Could this be a typographical error?

Thank you, this has been fixed.

Assuming σ_{β_m} and σ_{δ_m} are negligible and approximating $\sigma_R \approx \frac{\sigma_{\beta_p}}{\beta_m}$, this reduces to

$$\sigma^2_{\delta_p} \approx \left(\frac{\partial \delta_p}{\partial \delta_v}\sigma_{\delta_v}\right)^2 + \left(\frac{\partial \delta_p}{\partial R}\frac{\sigma_{\beta_p}}{\beta_m}\right)^2. \quad (1)$$

Additional instrumental effects not explicitly addressed:

a) The manuscript mentions the issue of overlap and refers to a correction methodology (Hervo et al., 2016), but this correction is not applied in the present analysis. Do the authors believe that the same technique developed for the CHM-15k could also be applied to the CL61 in order to separate the overlap contribution from other instrumental effects?

Hervo et al., 2016 is an example of how the internal temperature could affect the measurements. In this work, we demonstrated that the instrumental background bias and noise are also temperature dependent, and we presented a method for bias correction and uncertainty estimation based on the background characteristics.

b) Another issue not mentioned in the manuscript, which affected previous models of Vaisala ceilometers, is absorption by water vapor. According to the manufacturer, this issue has been mitigated by selecting a different wavelength and a very narrow bandwidth. Have the authors had the opportunity to verify this aspect in their measurements?

The finding by Looschelders et al. (2025) that calibration factors vary by less than 5% between CL61 instruments, coupled with the absence of seasonality in the calibration factor across all sites in this study (Fig. 6), indicate that the effect of water vapor is likely negligible on CL61.

Furthermore, we quantified the effect of water vapor absorption on CL61 by using the HITRAN molecular absorption database (Gordon et al., 2026). We compared two lidar systems: the CL51 with the emitted wavelength of 910 ± 1.44 nm (Wiegner and Gasteiger, 2015), and the CL61 with the emitted wavelength of 910.55 ± 0.08 nm, where the reported uncertainties correspond to the standard deviation ($\pm\sigma$) assuming Gaussian distributions. It should be noted that the information about the CL61 wavelength is not officially published, but only obtained through personal communication. Additionally, the transmitter from CL61 is identical to the non-water channel transmitter from the Vaisala DIAL lidar (personal communication) which operates at the same 910.55 nm wavelength, while its water channel is operating at a nearby wavelength of 910.99 nm (DA10 User Guide: https://docs.vaisala.com/r/M212895EN-E/en-US, last access: 10 June 2026). This further supports the much narrower width of the emission spectrum of CL61 compared to CL51. Given these assumptions, our analysis indicates that water vapor absorption reduces the two-way transmission in the CL51 by approximately a factor of 10 more than in the CL61. As the impact of atmospheric water vapor on the CL51 has previously been reported (Wiegner and Gasteiger, 2015), this result indicates that the effect of atmospheric water vapor absorption is minimal on the CL61.

3 Technical comments

Nomenclature: the CL61 is referred to both as a “ceilometer” and as an “elastic backscatter lidar” (e.g., line 1), seemingly interchangeably. In recent years, the term “Automatic Lidar-Ceilometer” has become increasingly common. The authors may wish to consider this terminology.

Thanks, this has been implemented.

Abstract: the first part mainly uses present tense verbs, whereas the second part switches to past tense. The authors may consider harmonizing the tense throughout the abstract.

The abstract has been updated:

The Vaisala CL61 is a new generation elastic backscatter lidar that extends conventional Automatic Lidar-Ceilometer capabilities by providing depolarization ratio measurements. Reliable use of these measurements, however, requires thorough evaluation and characterisation of the instrument performance and subsequent corrections applied. In this study, performance of multiple CL61 instruments across different sites over 3 years period have been assessed. Results indicate some differences between instruments, with most of these early production units exhibiting a pronounced decrease in laser power over time, accompanied by an increase in background noise likely due to weaker return signal. Normally, the instrument scales the internal calibration factor to compensate for changes in laser power and thus provide consistent attenuated backscatter coefficient values from profile to profile over time. However, for the instrument at the Lindenberg site, by performing manual calibration with atmospheric targets it is noted that once the laser power dropped below 40% *there is no further compensation in the internal calibration factor.*

The instrumental background noise and bias, characterized using the termination hood, are found to vary with temperature. A method has been developed for correcting the instrumental bias and for estimating the associated uncertainty. Additionally, an approach to estimate the uncertainty of volume and particle backscatter and linear depolarization ratio is presented. In a case study representing low aerosol load condition in Finland, the bias-corrected particle linear depolarization ratio has been found to deviate by up to 0.1 from the original instrument-provided volume linear depolarization ratio. This demonstrates the importance of accounting for the molecular contribution in both volume backscatter and linear depolarization ratio when quantitatively interpreting aerosol measurements by the CL61 Automatic Lidar-Ceilometer operating at the wavelength of $910.55\,\mathrm{nm}$*. Finally, signal loss in one unit has been traced to fogging of the inside surface of the window, and attributed to insufficient internal heating linked to the instrument’s firmware behavior.*

Line 4: can background noise appropriately be referred to as a “signal”? In addition, two rather different issues are mentioned consecutively: the quantification of background noise and calibration using liquid clouds. It might be better to separate these two aspects more clearly.

Thanks, the correct term “background noise” has been used. As recommended also by the Reviewer 2, the methodological details, namely the quantification of background noise and the calibration using liquid clouds, have been removed from this section to place greater focus on the results.

In this study, performance of multiple CL61 instruments across different sites over 3 years period have been assessed. Results indicate some differences between instruments, with most of these early production units exhibiting a pronounced decrease in laser power over time, accompanied by an increase in background noise likely due to weaker return signal.

Line 4: “long-term behavior” is somewhat generic and could be specified more precisely. The same applies to “variability” in line 5.

Changed “long-term behavior” to ”performance .. over 3 years” and ”variability” to ”differences”. See the answer above.

Lines 12–14: the approach used for aerosol inversion and the calculation of the depolarization ratio are not entirely novel. Rather, the contribution of the paper could be emphasized in terms of the uncertainty propagation in the inversion and in the depolarization ratio retrieval.

We have modified lines 12–14 as following:

A method has been developed for correcting the instrumental bias and for estimating the associated uncertainty. Additionally, an approach to estimate the uncertainty propagation of volume and particle backscatter and linear depolarization ratio is presented.

Line 14: after “accounting for molecular contribution”, it would be clearer to add “both in the aerosol backscatter and in the depolarization ratio”.

This demonstrates the importance of accounting for the molecular contribution in both backscatter and linear depolarization ratio when qualitatively interpreting aerosol measurements by the CL61 Automatic Lidar-Ceilometer operating wavelength of 910.55 nm

Line 50: does the “optical path” referred to here correspond to the optical path inside the instrument?

We changed it to "temperature sensitivity of the instrumental background" to encompass both the optical and the electronics.

Our analysis focuses on the impact of laser power on signal quality, the temperature sensitivity of the instrumental background and methods for its correction.

Equations (1), (2), and (3): in Eq. (1), defining B as the background noise appears correct. However, in the subsequent equations, if p_{pol} and x_{pol} represent the signals provided by the instrument firmware, then B should represent the firmware estimate—rather than the exact value—of the background noise, as described in the following sections.

Thank you, this has been implemented. Instrument estimated background noise $B_{estimate}$ and residual background noise B_{res} have been introduced. Line 91 has been modified as:

where $B_{\mathrm{estimated}}$ *is the internally estimated background signal by the instrument.*

Line 100 to 105 has been modified as:

Although the instrument already determines and performs the background correction internally, residual background components may still remain in the measured signal, such as the dark signal observed during termination hood measurements (see Sect 3.1.1). Therefore, we extend Eqs. 2 and 3 to account for the residual background signal (hereafter referred to as the background signal), B_{res}, *that is not removed by the internal correction:*

Section 3.1: it might be clearer to title the section “Residual background noise”, since a first correction is already applied by the firmware. Similarly, in line 103, it might be useful to specify “unaccounted background terms”.

Thanks for the suggestion, the title of the section has been modified to "Residual background noise". See the previous reply for the additional introduction of $B_{estimate}$ and B_{res}.

Line 97: please specify what the two letters "bk" stand for, given that B already denotes "background".

Thank you, "bk" has been removed and B has been separated as instrument estimated background noise $B_{estimate}$ and residual background noise B_{res}. See previous reply for more detail

Lines 110–115: does this description uniquely (and reproducibly) define the procedure followed? In particular, the exact PyWavelets wavelet identifier (e.g., bior1.1), the definition of the minimax threshold and the method used for noise variance estimation, the treatment of approximation coefficients, and the exact threshold computation used for noise-gate identification should be clarified.

The text in lines 110–115 provides sufficient detail to reproduce the method. The minimax threshold is applied in the wavelet decomposition to reduce noise in the signal by minimizing the maximum mean squared error across the wavelet coefficients. Both the threshold computation and the wavelet decomposition can be readily implemented using PyWavelets python package following the described procedure.

The following has been added:

The mean and variance of the background are computed from the original, non-averaged data with the identified background range gates using 5-minute time intervals and 2 km range-bin intervals.

Line 133: if I am not mistaken, the terms μ have not been introduced previously and should therefore be defined.

These terms have been introduced as following in line 130:

During daylight hours, solar radiation significantly increases the variance ($\sigma^2{}_{\parallel P_{\mathrm{res}}}$ and $\sigma^2{}_{\perp P_{\mathrm{res}}}$) of the background signal, resulting in a daytime variance much higher than that observed at night, as shown in panels (g) and (h). Above the aerosol and cloud layers, both the mean ($\mu_{\parallel P_{\mathrm{res}}}$ and $\mu_{\perp P_{\mathrm{res}}}$) and variance of the background signals in both polarizations remain relatively stable with range, or at least exhibit considerably smaller variations compared to the diurnal fluctuations.

Figure 3, caption: the caption reports σ_{ppol}/r^2, whereas the axis in the figure shows σ^2_{ppol}/r^2.

Thank you, the figure axis labeled has been corrected as σ^2_{ppol/r^2}

Line 149: when referring to the instrument temperature, in what part of the instrument is it measured? It should be clarified whether this corresponds to the module temperature, the internal temperature, or specifically the laser temperature.

Thank you, this has been implemented.

To quantify the effect of temperature, the termination hood measurement was repeated over a range of internal temperatures T, reported as `internal_temperature` in the instrument housekeeping data, across a two-year period.

Section 3.1.2: please clarify whether the calculation of P_{solar} is performed for each individual profile.

This is performed for each individual profile.

Here, $\sigma^2_{P_{atmosphere}}$ is independent of the range and is obtained separately for each polarization in each individual profile.

Line 155: is σ^2 uniform, or σ^2/r^2?

$\sigma^2{}_{P_{atmosphere}}$ is uniform which is the $\sigma^2{}_{\frac{ppol}{r^2}}$ and $\sigma^2{}_{\frac{xpol}{r^2}}$ in the background range gates.

Line 162: I believe the reference should be to Figs. 3b and 3c, rather than 2b/2c.

Thank you for spotting the mistake, this has been fixed

Lines 205–209: additional detail may be helpful here. How is the example profile selected? Presumably the cross-correlation accounts for possible shifts in cloud altitude (or other profile characteristics)? Which exact quantity is correlated along the profile (e.g., β')?

This has been reformulated to include more details:

A methodology was developed to identify suitable liquid cloud profiles. First, a representative liquid cloud profile containing a single liquid cloud layer and exhibiting complete signal attenuation approximately 200 m above the cloud base was selected as the reference profile. Each ppol *profile in the dataset was then cross-correlated with this reference to quantify their similarity. For each time step, the height corresponding to the maximum cross-correlation value was identified as the most similar location and treated as a pseudo in-cloud height. Next, the ratio of total in-cloud β', calculated over a 150 m layer centered at the pseudo in-cloud height, to the integrated β' of the entire profile was computed. A profile was classified as containing a liquid cloud if this ratio exceeded 90%, ensuring that the integrated β' was not significantly influenced by strong aerosol loading or precipitation. Additionally, the cross-correlation value at the identified height was required to exceed 5×10^{-7}. This threshold was selected to ensure that at least 1000 valid data points were available for each month.*

Line 252: it might be useful to specify that the normalization assumes Poisson statistics.

Thanks, this has been implemented

Figure 4 shows the time series of background noise (variance of the background signal), normalized by integration time assuming Poisson statistics ($\sigma^2_{ppol/r^2} \times t_{intergration}$), alongside the laser power.

Sections 4.2 and 4.3: in the description of the figures (e.g., line 282 onward; line 311 onward), the text refers to station names. However, if the reader wants to identify the corresponding panel, they must read the figure caption and match the station name with the subfigure label (a, b, c, . . .). It would be more convenient either to refer directly to the subfigure in the main text or to include the station name in each subfigure title.

Thanks, this has been implemented to include the station name.

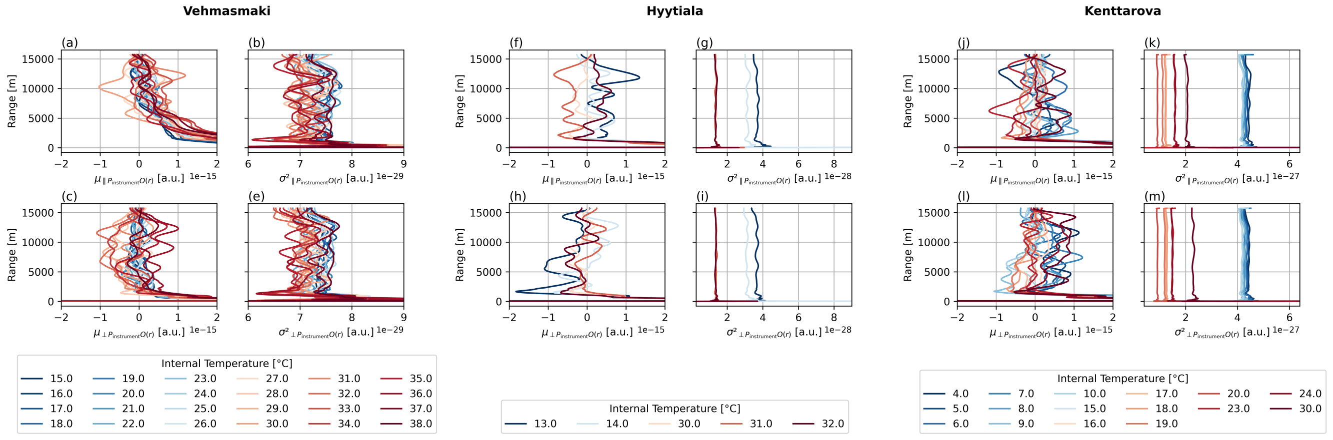

Figure 6. *Termination hood profiles at various internal temperatures (color-coded) across different sites. In Vehmasmaki: a) $\mu_{\parallel P_{\mathrm{instrument}} O(r)}$, b) $\sigma_{\parallel P_{\mathrm{instrument}} O(r)}$, c) $\mu_{\perp P_{\mathrm{instrument}} O(r)}$, and d) $\sigma_{\perp P_{\mathrm{instrument}} O(r)}$. In Hyytiala: f) $\mu_{\parallel P_{\mathrm{instrument}} O(r)}$, g) $\sigma_{\parallel P_{\mathrm{instrument}} O(r)}$, h) $\mu_{\perp P_{\mathrm{instrument}} O(r)}$, and i) $\sigma_{\perp P_{\mathrm{instrument}} O(r)}$. In Kenttärova: j) $\mu_{\parallel P_{\mathrm{instrument}} O(r)}$, k) $\sigma_{\parallel P_{\mathrm{instrument}} O(r)}$, l) $\mu_{\perp P_{\mathrm{instrument}} O(r)}$, and m) $\sigma_{\perp P_{\mathrm{instrument}} O(r)}$*

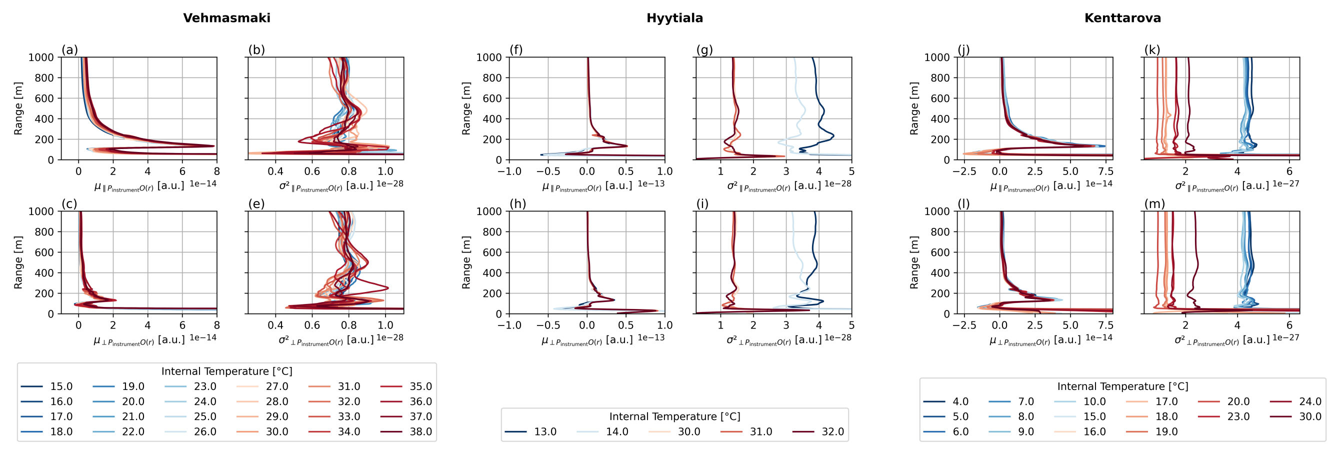

Figure 7. *Termination hood profiles at various internal temperatures (color-coded) across different sites only up to 1000 m range. In Vehmasmaki: a) $\mu_{\parallel P_{\mathrm{instrument}} O(r)}$, b) $\sigma_{\parallel P_{\mathrm{instrument}} O(r)}$, c) $\mu_{\perp P_{\mathrm{instrument}} O(r)}$, and d) $\sigma_{\perp P_{\mathrm{instrument}} O(r)}$. In Hyytiala: f) $\mu_{\parallel P_{\mathrm{instrument}} O(r)}$, g) $\sigma_{\parallel P_{\mathrm{instrument}} O(r)}$, h) $\mu_{\perp P_{\mathrm{instrument}} O(r)}$, and i) $\sigma_{\perp P_{\mathrm{instrument}} O(r)}$. In Kenttärova: j) $\mu_{\parallel P_{\mathrm{instrument}} O(r)}$, k) $\sigma_{\parallel P_{\mathrm{instrument}} O(r)}$, l) $\mu_{\perp P_{\mathrm{instrument}} O(r)}$, and m) $\sigma_{\perp P_{\mathrm{instrument}} O(r)}$.*

Lines 292–293: if I am not mistaken, the temperature dependence in subfigures 6k and 6m appears to reverse at some point. Are the authors able to explain this inversion?

Yes, it is due to the noise introduced by the internal heater when the internal temperature falls below an instrument-specific threshold (15 °C for Hyytiälä and Kenttärova). The following has been added to the text.

These instrumental background noise profiles show a pronounced sensitivity to internal temperature (from 4°C to 38°C). Notably, very low temperatures are associated with elevated instrumental background noise across the entire measurement range. This can be explained by the effect of the internal heater. As the internal temperature falls below an instrument-specific threshold (15 °C for Hyytiälä and Kenttärova), the internal heater is turned on. This leads to an increase in $\sigma^2_{P_{\mathrm{instrument}}O(r)}$*, with the effect becoming more pronounced as the temperature decreases. When the internal temperature is high and the internal heater is off, internal temperature positively correlates with* $\sigma^2_{P_{\mathrm{instrument}}O(r)}$.

Figure 6: the subfigures do not appear to be vertically aligned.

Thanks, this has been fixed, see the reply above.

Line 339: the quantities referred to as “values” are actually differences, correct?

Thanks, “values” has been changed to difference.

In below $1000\ \mathrm{m}$ *range, the corrected* β'_v *differs only slightly from the original uncorrected* β'*, with the difference ranging from* 1×10^{-9} *to* $2.5 \times 10^{-9}\ \mathrm{sr}^{-1}\ \mathrm{m}^{-1}$

Lines 351–354: is there a physical reason why σ_δ depends on signal intensity, whereas this does not appear to be the case for σ_β? Could the authors provide an intuitive explanation?

The uncertainties of $xpol$ and $ppol$ are of the same order of magnitude. However, the absolute values of $ppol$ are much larger than those of $xpol$. As a result, the small uncertainty in $xpol$ can lead to a relatively large uncertainty in δ. The figure has been updated with an improved color scale for better visualization. Additionally, the uncertainty propagation for β now includes a 10% uncertainty associated with the calibration factor, which further increases σ_δ depending on the signal intensity.

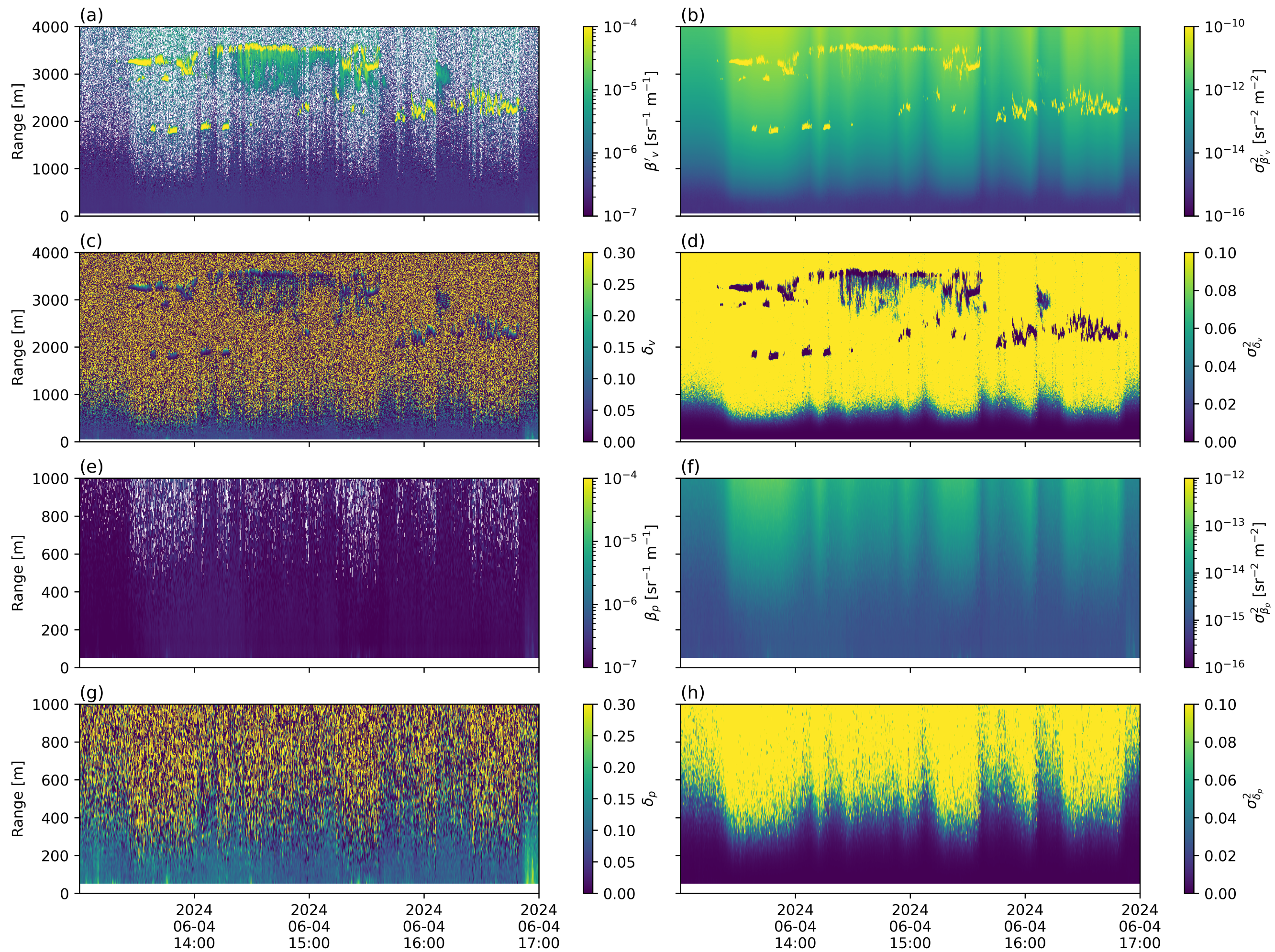

Figure 11. *An example of corrected profile in Kenttärova on 2024-06-04 13:00 - 17:00 UTC (same day as Fig. 10). a) β'_v, b) $\sigma^2_{\beta'_v}$ c) δ_v, d) $\sigma^2_{\delta_v}$ e) β_p, f) $\sigma^2_{\beta_p}$, g) δ_p, and h) $\sigma^2_{\delta_p}$.*

Lines 368–369: could the authors indicate how the blower and heater are configured to remain permanently on?

The blower and heater cannot be configured to remain permanently on.

This issue could be mitigated by keeping both the window blower and heater always on. However, at the time of this writing, this is not possible (personal communication with Vaisala).

Figure 11: how does relative humidity (RH) behave inside the instrument under these conditions?

Thanks, this has been added to the graph. The relative humidity was at below 70%. However, because the outside temperature was much colder and the window blower heater was turned off, condensation formed on the inside surface of the window.

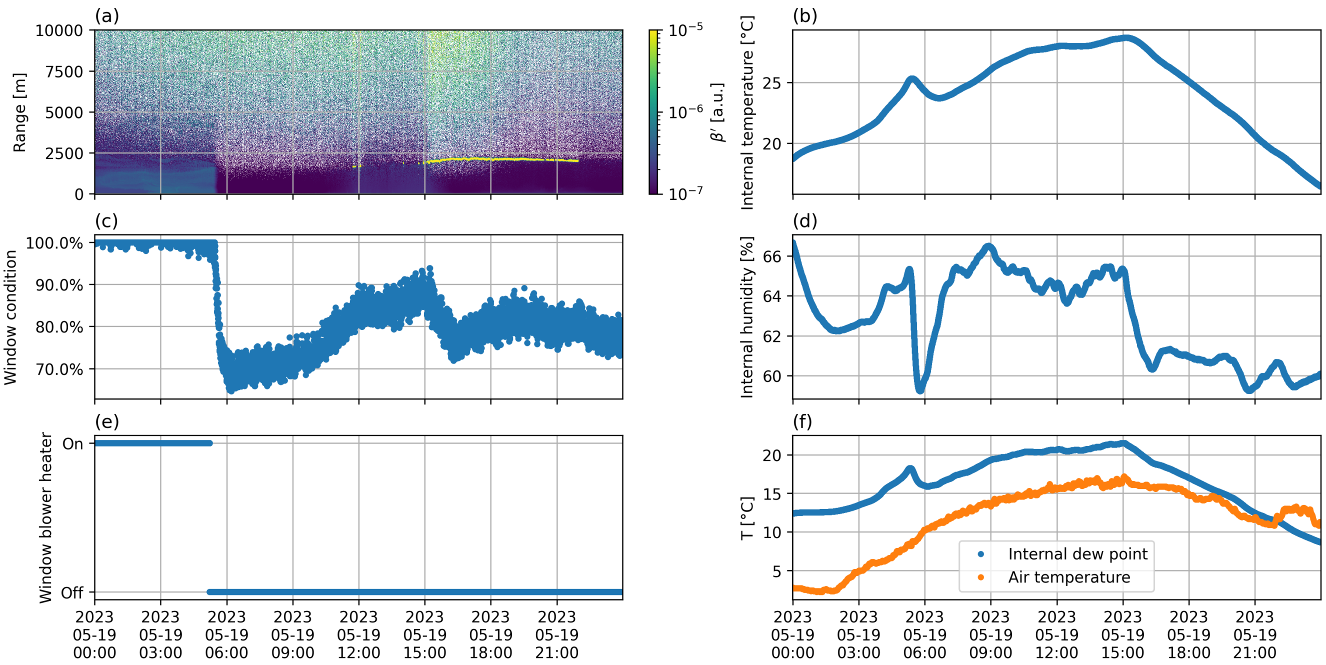

Figure 12. *Measurements from Vehmasmäki on 2023-05-19 a) β', b) Internal temperature, c) window condition, d) Internal humidity, e) Window blower heater, f) Calculated dew point and measured outside air temperature*

Conclusions: Lines 372–373: please clarify what results are specific to the CL61.

In this study, we quantify the temporal variability of background noise and calibration factors for the CL61 across multiple sites over a three-year period using methodologies adapted from existing approaches.

Line 381: since the Klett inversion depends on the signal at lower altitudes, measurements affected by the discussed issue should probably be discarded or replaced (e.g., with the immediately higher range gates) not only in the final results but also within the inversion calculation itself.

This has been added to the method:

The first 50 m range has been discarded due to unreliable data (see Sect. 4.5), and it has been demonstrated that the resulting loss in optical depth for ignoring near range gates is negligible (Wiegner and Geiß, 2012).

References

Gordon, I. E., Rothman, L. S., Hargreaves, R. J., Gomez, F. M., Bertin, T., Hill, C., Kochanov, R. V., Tan, Y., Wcisło, P., Makhnev, V. Y., Bernath, P. F., Birk, M., Boudon, V., Campargue, A., Coustenis, A., Drouin, B. J., Gamache, R. R., Hodges, J. T., Jacquemart, D., Mlawer, E. J., Nikitin, A. V., Perevalov, V. I., Rotger, M., Robert, S., Tennyson, J., Toon, G. C., Tran, H., Tyuterev, V. G., Adkins, E. M., Barbe, A., Bailey, D. M., Bielska, K., Bizzocchi, L., Blake, T. A., Bowesman, C. A., Cacciani, P., Čermák, P., Császár, A. G., Denis, L., Egbert, S. C., Egorov, O., Ermilov, A. Y., Fleisher, A. J., Fleurbaey, H., Foltynowicz, A., Furtenbacher, T., Germann, M., Guest, E. R., Harrison, J. J., Hartmann, J. M., Hjältén, A., Hu, S. M., Huang, X., Johnson, T. J., Jóźwiak, H., Kassi, S., Khan, M. V., Kwabia-Tchana, F., Lee, T. J., Lisak, D., Liu, A. W., Lyulin, O. M., Malarich, N. A., Manceron, L., Marinina, A. A., Massie, S. T., Mascio, J., Medvedev, E. S., Meshkov, V. V., Mellau, G. C., Melosso, M., Mikhailenko, S. N., Mondelain, D., Müller, H. S. P., O'Donnell, M., Owens, A., Perrin, A., Polyansky, O. L., Raston, P. L., Reed, Z. D., Rey, M., Richard, C., Rieker, G. B., Röske, C., Sharpe, S. W., Starikova, E., Stolarczyk, N., Stolyarov, A. V., Sung, K., Tamassia, F., Terragni, J., Ushakov, V. G., Vasilchenko, S., Vispoel, B., Vodopyanov, K. L., Wagner, G., Wójtewicz, S., Yurchenko, S. N., and Zobov, N. F.: The HITRAN2024 molecular spectroscopic database, Journal of Quantitative Spectroscopy and Radiative Transfer, 353, 109 807, https://doi.org/10.1016/j.jqsrt.2026.109807, 2026.

Looschelders, D., Christen, A., Grimmond, S., Kotthaus, S., Fenner, D., Dupont, J.-C., Haeffelin, M., and Morrison, W.: Inter-Instrument Variability of Vaisala CL61 Lidar-Ceilometer's Attenuated Backscatter, Cloud Properties and Mixed-Layer Height, Meteorological Applications, 32, e70 088, https://doi.org/10.1002/met.70088, _eprint: https://rmets.onlinelibrary.wiley.com/doi/pdf/10.1002/met.70088, 2025.

Wiegner, M. and Gasteiger, J.: Correction of water vapor absorption for aerosol remote sensing with ceilometers, Atmospheric Measurement Techniques, 8, 3971–3984, https://doi.org/10.5194/amt-8-3971-2015, publisher: Copernicus GmbH, 2015.

Wiegner, M. and Geiß, A.: Aerosol profiling with the Jenoptik ceilometer CHM15kx, Atmospheric Measurement Techniques, 5, 1953–1964, https://doi.org/10.5194/amt-5-1953-2012, 2012.

Response to reviewer 2's comments for Operational performance of the Vaisala CL61 ceilometer for atmospheric profiling

Viet Le[1], Ewan J. O'Connor[1], Maria Filioglou[2], and Ville Vakkari[1, 3]

[1]Finnish Meteorological Institute, Helsinki, 00101, Finland
[2]Finnish Meteorological Institute, Atmospheric Research Centre of Eastern Finland, Kuopio, Finland
[3]Atmospheric Chemistry Research Group, Chemical Resource Beneficiation, North-West University, Potchefstroom, 2520, South Africa

Correspondence: viet.le@fmi.fi

We would like to thank the reviewers for the constructive comments. Below are the reviewer comments in black text, followed by our responses in blue text. Where applicable, we also provide changes to the manuscript in *blue italics*.

1 General comments

This manuscript presents a long-term evaluation of the Vaisala CL61 depolarization ceilometer using measurements from four ACTRIS Cloudnet sites in Finland and Germany. The study addresses several important aspects of the operational performance of this new-generation ceilometer, including background noise characterization, laser power degradation, temperature-dependent instrument bias, calibration stability, and the retrieval of aerosol backscatter and depolarization profiles.

The topic is timely and relevant. Depolarization-capable ceilometers are increasingly used in operational networks, and the CL61 represents an important step toward extending ceilometer applications to aerosol typing and cloud microphysics. A careful characterization of instrument performance under long-term operation is therefore essential for both operational and research communities. The manuscript contains several interesting aspects, such as the use of termination hood measurements to quantify instrumental noise and the comparison of cloud and Rayleigh calibration approaches.

Overall, the manuscript is reasonably well structured and generally clear, although the organization could be improved in some parts. Several methodological aspects require clarification, and some conclusions appear stronger than what is fully supported by the presented evidence. I therefore recommend publication after major revisions addressing the points outlined below.

We would like to thank the reviewer for their positive evaluation of the manuscript.

2 Specific comments

The manuscript would benefit from a clearer separation and description of the different signal components relevant to lidar measurements (true atmospheric signal, background signal, instrumental dark signal) and their associated noise contributions in the methods section. It should also be clarified which components are corrected by the instrument firmware and which require additional processing addressed in this study. The lidar equation presented in Section 2 would be more appropriately placed in this part of the paper.

The background definition B has been improved. Now it is consists of estimated background signal $B_{estimated}$ by the instrument and residual background signal B_{res}. The residual background signal consists of atmospheric background signal (such as solar) and instrumental background signal (dark signal). The study examines the instrumental background signal and its associated noise. The atmospheric background signal has been corrected by the firmware, its variance (atmospheric background noise) will be addressed in this study.

Here are the updated paragraphs across the manuscript:

$$ppol =^{\parallel} \frac{(P(r) - B_{\text{estimated}})r^2}{C_L O(r)} =^{\parallel} \beta', \tag{1}$$

$$xpol =^{\perp} \frac{(P(r) - B_{\text{estimated}})r^2}{C_L O(r)} =^{\perp} \beta', \tag{2}$$

where $B_{\text{estimated}}$ is the internally estimated background signal by the instrument.

...Although the instrument already determines and performs the background correction internally, residual background components may still remain in the measured signal, such as the dark signal observed during termination hood measurements (see Sect 3.1.1). Therefore, we extend Eqs. 2 and 3 to account for the residual background signal (hereafter referred to as the background signal), B_{res}, that is not removed by the internal correction:...

...Therefore, the firmware must have corrected the atmospheric background signal to a zero mean, leaving only its variance (noise) contributing to the background signal, which will be addressed in this study...

...During the termination hood measurement, $\mu_{P_{\text{instrument}}O(r)}$ from both polarizations remains relatively stable above $1.2\ \text{km}$, but increases significantly below this range (Figs. 3d, e). This increase suggests the presence of a signal bias at lower ranges that has not been corrected by the firmware and will be investigated in this study....

In addition, a clearer distinction between signal and noise is required throughout the manuscript, as these terms are occasionally used interchangeably, which may lead to confusion.

Thanks, this has been incorporated into the manuscript. An example is shown in lines 172-173:

Hence, the instrumental background signal mean (bias) and its variance (noise) from both polarizations with respect to internal temperature can be determined.

It is currently not clear whether the instrumental correction (dark signal) s negligible when compared to real atmospheric measurements. The manuscript would benefit from a quantitative assessment of the magnitude of the instrumental signal relative to the atmospheric signal, as well as a discussion of whether this contribution can be neglected and over which range.

Thanks, the following plots have been added to the supplements. Additionally, additional text to describe this is included in the manuscript.

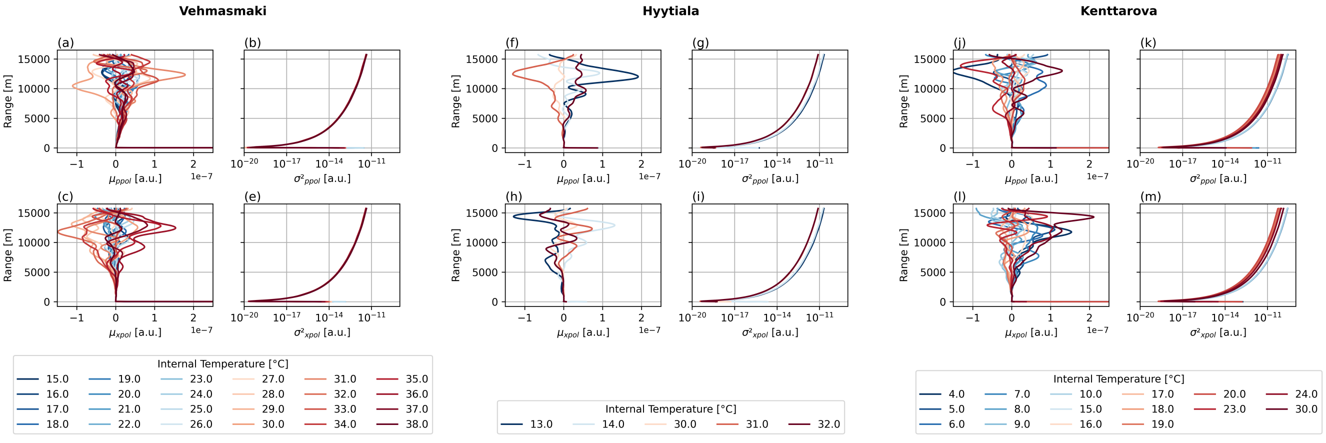

Figure S4. *Termination hood profiles at various internal temperatures (color-coded) across different sites. In Vehmasmaki: a) μ_{ppol}, b) σ^2_{ppol}, c) μ_{xpol}, and d) σ^2_{xpol}. In Hyytiala: f) μ_{ppol}, g) σ^2_{ppol}, h) μ_{xpol}, and i) σ^2_{xpol}. In Kenttärova: j) μ_{ppol}, k) σ^2_{ppol}, l) μ_{xpol}, and m) σ^2_{xpol}*

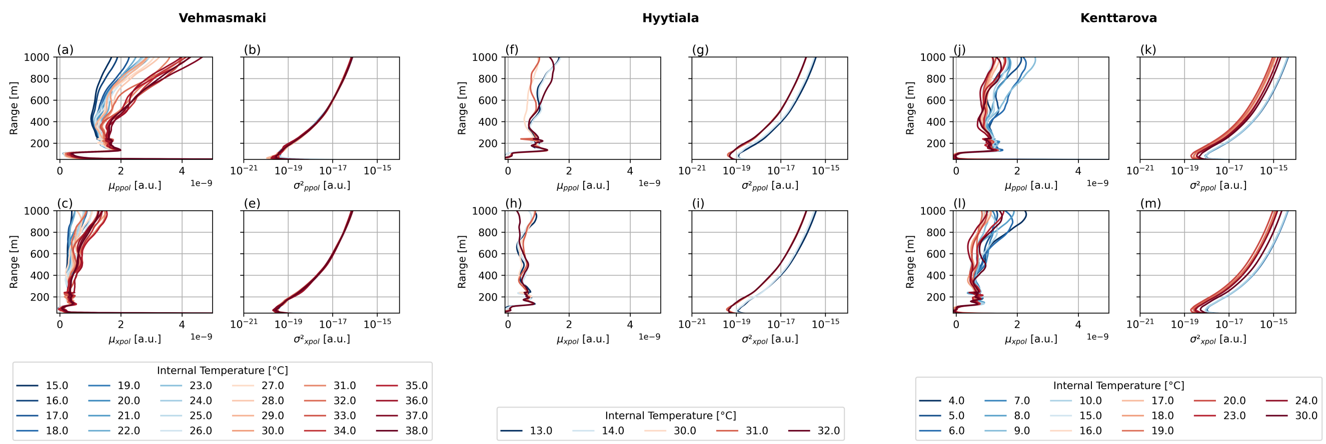

Figure S5. *Termination hood profiles at various internal temperatures (color-coded) across different sites only up to 1000 m range. In Vehmasmaki: a) μ_{ppol}, b) σ^2_{ppol}, c) μ_{xpol}, and d) σ^2_{xpol}. In Hyytiala: f) μ_{ppol}, g) σ^2_{ppol}, h) μ_{xpol}, and i) σ^2_{xpol}. In Kenttärova: j) μ_{ppol}, k) σ^2_{ppol}, l) μ_{xpol}, and m) σ^2_{xpol}.*

Similar to Figs. 6 and 7, Figs. S4 and S5 show the same profiles obtained during the termination hood measurements, but include range correction and the instrument-provided overlap correction. These profiles of ppol and $xpol$ provide a direct quantification of the impact of instrumental background bias and noise on the measurements and their dependence on temperature. For all CL61 instruments, the instrumental biases, μ_{ppol} and μ_{xpol}, remain below the order of 10^{-7}, while the noise terms, σ^2_{ppol} and σ^2_{xpol}, remain below the order of 10^{-11}. These biases are even smaller below 5 km. Below a range of 1 km, μ_{ppol} remains below 5×10^{-9} and μ_{xpol} below 3×10^{-9}. These small biases are usually negligible comparing to the typical atmospheric signal. However, at very clean sites such as Kenttärova, the instrumental bias in $xpol$ can still affect

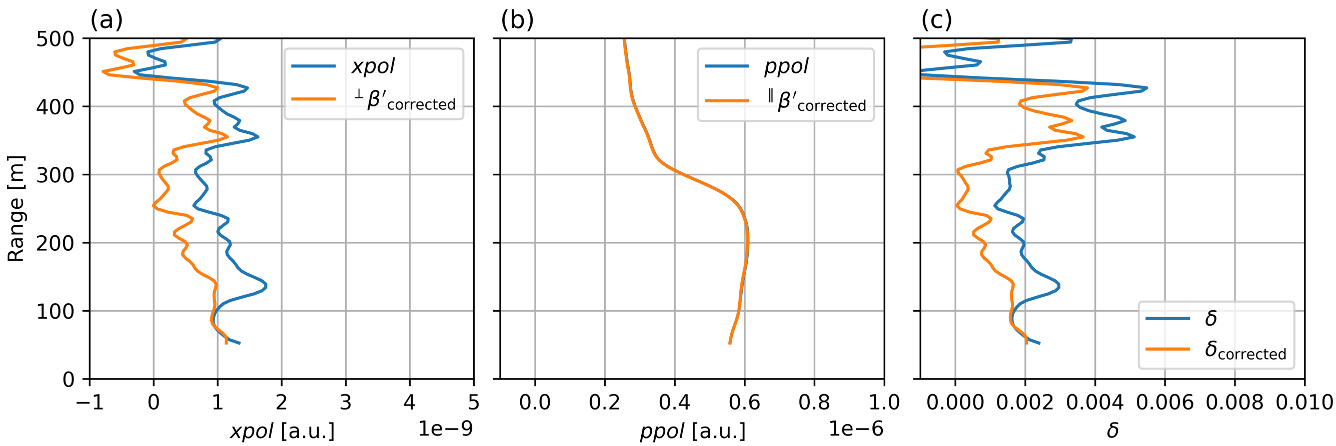

Figure S6. *Data from Kenttärova 2023-10-03, averaged from 11:00 to 15:00 UTC showing a) $xpol$, b) $ppol$ c) δ.*

the retrieved aerosol depolarization ratio, particularly under conditions of low depolarization. An example is shown in Fig. S6, which presents measurements from Kenttärova on 2023-10-03 under weakly depolarizing aerosol conditions. During this period, the $xpol$ profile below $400\ \mathrm{m}$ is on the order of 10^{-9}, while $ppol$ remains on the order of 10^{-6}. As a result, the instrumental bias becomes relatively significant for $xpol$, leading to a noticeable, although quantitatively small, reduction in δ (from 0.002 to 0.001 at $200\ \mathrm{m}$) after the bias correction is applied. Furthermore, the previously mentioned peak at $150\ \mathrm{m}$ is clearly visible in this case and is effectively mitigated after the removal of the instrumental bias.

Some statements, for example regarding the recommended frequency of termination hood measurements, are not clearly supported by the presented results. This information would be particularly important for instrument operators, given the associated effort.

We modified our suggestion as following:

Figure 8 shows how the instrumental bias during the termination hood measurement at Vehmasmäki varies over time under consistent internal temperature conditions. Over a six-month period, the calibration profiles at each temperature show only minor fluctuations. Therefore, we recommend performing termination hood checks at least once across the operating temperature range to determine the instrumental background signal bias and noise.

In addition, the temperature-dependent overlap behaviour mentioned in the conclusions cannot be clearly inferred from the data shown.

As also noted by referee 1, we modified it to be the temperature dependence of the instrumental background bias and noise. This temperature dependence is shown in Fig. 6 and Fig. 7, and even more clearly in Fig. S4 and Fig. S5 below 1 km without the range and overlap correction.

Termination hood measurements were performed on selected instruments and proved effective in characterizing the instrumental background bias and noise profiles and and their temperature dependence.

3 Technical comments

Line 1: Within the community, the term ALC has become established as standing for ‘Automatic Low-Power Lidar and Ceilometer’ or ‘Automatic Lidar-Ceilometer’. Perhaps the authors also wish to use this term to distinguish them from aerosol high-power lidars (AHL).

Thanks, we will follow the suggestion.

The Vaisala CL61 is a new generation elastic backscatter lidar that extends conventional Automatic Lidar-Ceilometer capabilities by providing depolarization ratio measurements.

Line 4: In this context, the focus should not be placed on the introduction of methods, as these are already well established in the lidar community, but rather on the adaptation and application of existing methods to long-term CL61 data, which represents a key contribution of this manuscript.

Changed the sentence to emphasize on the assessment of the CL61s.

In this study, performance of multiple CL61 instruments across different sites over 3 years period have been assessed.

Line 6: Does this refer to an increase in noise due to e.g. changes in detector characteristics or a decrease in the signal-to-noise ratio due to weaker return signals?

It is due to a decrease in signal-to-noise ratio due to weaker return signals, and the instrument’s compensation via internal calibration factor

Results indicate some differences between instruments, with most of these early production units exhibiting a pronounced decrease in laser power over time, accompanied by an increase in background noise likely due to weaker return signal

Line 11: A variation is obvious for the instrumental noise but is it also true for the bias?

Yes, it is. An example is in Fig. 7f and 7h, where cold temperature introduces negative bias in the near range. This is even more clear in the newly added Fig. S4 and Fig. S5.

Line 13: A commonly used term would be the particle backscatter coefficient and the particle linear depolarization ratio (PLDR).

Thanks, i will follow the suggestion.

Additionally, an approach to estimate the uncertainty propagation of volume and particle backscatter and linear depolarization ratio is presented.

Line 17: The correct wavelength of the CL61 according to the manual is 910.55 nm.

Thanks, i will follow the suggestion.

This demonstrates the importance of accounting for the molecular contribution in both volume backscatter and linear depolarization ratio when qualitatively interpreting aerosol measurements by the CL61 Automatic Lidar-Ceilometer operating at the wavelength of 910.55 nm.

Line 23: Shouldn’t it be attenuated

Yes, it is attenuated backscatter as shown in the manuscript.

Line 28: An essential point here is eye-safety

Thanks, i will follow the suggestion.

Their ability to operate autonomously and reliably in challenging environmental conditions, as well as being eye-safe, makes them well-suited for long-term monitoring and integration into operational networks of national meteorological services and research institutions...

Line 33: volume linear depolarization ratio (VLDR) δ_v

Thanks, i will follow the suggestion.

Vaisala has recently introduced the CL61 ceilometer which is an ALC with the capability of measuring the volume linear depolarization ratio, δ_v, which is the ratio of the perpendicular to the parallel component of the backscattered signal relative to the emitted polarization.

Line 46: As lidars have a blind zone or a difficult to correct range of incomplete overlap, it is in principle impossible to obtain reliable data all the way down to the surface.

With monostatic systems such as the CL61 reliable data can be extended much closer to surface compared to most research-grade lidars. Here, we consider surface as heights that can be covered with standard masts, i.e. 50 - 100 m above ground.

Identifying and correcting such artifacts in the CL61 would enable reliable observations extending down to heights that overlap with surface-based observations.

Line 50: Is it the optical path or rather the detector or transmitter unit which is temperature dependent?

We think it is the combinations of those. Hence, we reprhase the sentence to say it is due to temperature dependent of the instrumental background signal as:

Our analysis focuses on the impact of laser power on signal quality, the temperature sensitivity of the instrumental background,..

Table 1: An additional important information is the telescope field of view and the height of complete overlap or the blind zone which is shortly mentioned in the text.

Thanks, i will follow the suggestion. I added Fig. S1 about the overlap function in the supplement and added description in the text:

The overlap functions are shown in Fig. S1. Full overlap between the transmitted laser beam and the receiver field of view is achieved at approximately $250\ \mathrm{m}$ *range for the instrument at Kenttärova. The instruments at Vehmasmaki and Hyytiälä have different overlap functions, with approximately 95% overlap at* $250\ \mathrm{m}$ *range and complete overlap at approximately* $550\ \mathrm{m}$ *range. The overlap function is reported only in the new firmware data and remains constant throughout the period. No overlap function was reported for the instrument at Lindenberg.*

Line 59: The manual states: attenuating acquisition for both signals with measurement time of 0.2 s and same receiver module is used for both signals. This means that receiver sensitivity calibration is not necessary.

Thanks, this information has been added to the text as suggested:

The CL61 alternates the acquisition of each polarization every $0.2\ \mathrm{s}$*, while using the same receiver module for both channels. Consequently, receiver sensitivity calibration is not required.*

Line 71: pulses of linear polarized laser light

Thanks, i will follow the suggestion.

In brief, the CL61 utilizes an InGaAs diode laser that emits linearly polarized pulses with an energy of $3.9\ \mu\mathrm{J}$ *at a repetition rate of* $9.5\ \mathrm{kHz}$

Line 73: Is B the background noise or the sum of additional signal terms like background and dark signal?

The B term is the sum of all the background components in this equation. The B term has been clarified later as estimated background signal by the instrument $B_{estimated}$ and residual background signal B_{res}

Line 88: linear depolarization ratio

Thanks, i will follow the suggestion.

and the volume linear depolarization ratio being:

Line 92-94: In line 4, it was referred to as a background signal, which is more accurate, as the background signal does indeed have a mean value and is not merely noise.

Thanks, i will follow the suggestion and make the term noise and signal more clear throughout the whole text. Please see the previous reply in the Section 2 of this reply regarding this.

Line 94: Authors should clearly distinguish between the components of the measured lidar signal and label them correctly. The measured signal consists of the true atmospheric signal plus the background signal, which may be caused by solar radiation, but also by moonlight or artificial light. Added to this is the instrument-specific signal, which may also be referred to as the 'dark signal' and can be determined, for example, through termination hood measurements.

Thanks, i will follow the suggestion and make the term noise and signal more clear throughout the whole text. Please see the previous reply in the Section 2 of this reply regarding this.

The true atmospheric signal consists of backscattered contributions from particles (β_p*) and molecular scattering (*β_{mol}*), whilst the background signal includes contributions from both atmospheric background signal* $P_{atmosphere}$ *(such as solar radiation, moonlight, or artificial light) and instrumental background* $P_{instrument}$ *signal (dark signal).*

Line 95: The firmware already subtracts the background signal, but not the dark signal. Do the authors also assume that the background signal was not correctly determined and subtracted? If so, they should refer to it as the residual background signal and dark signal (determined with termination hood measurements).

Thanks, I will follow the suggestion and refer to it as the residual background signal. As explained in a later section, the atmospheric background signal was assumed to have been correctly determined and corrected. However, the atmospheric background noise remains present and is incorporated with the instrumental background noise into the uncertainty estimation.

Line 97: Can B_{bk} be described as the dark signal in this context?

This has been clarified in the text. The total background signal is B, of which the estimated background from the instrument is $B_{estimated}$ and the residual background signal is B_{res}

...where $B_{\mathrm{estimated}}$ *is the internally estimated background signal by the instrument...*

...Therefore, we extend Eqs. 2 and 3 to account for the residual background signal (hereafter referred to as the background signal), B_{res}*, that is not removed by the internal correction:...*

Line 105: Background signal is usually range independent and dark signal range dependent. Since the solar component is specified here, is this then an uncorrected residual component?

No, the solar background signal mean is zero; however, the solar background noise remains substantial and is used to estimate the uncertainty, as shown in Eqs. 12–15.

Figure 1: Have σ and η for ppol and xpol been introduced yet?

Thanks, this has been added.

During daylight hours, solar radiation significantly increases the variance ($\sigma^2{}_{ppol/r^2}$ and $\sigma^2{}_{xpol/r^2}$) of the background signal, resulting in a daytime variance much higher than that observed at night, as shown in panels (g) and (h). Above the aerosol and cloud layers, both the mean (μ_{ppol/r^2} and μ_{xpol/r^2}) and variance of the background signals in both polarizations remain relatively stable with range, or at least exhibit considerably smaller variations compared to the diurnal fluctuations.

Line 131: To obtain the correct dark signal the overlap correction must be removed. It is still applied in the firmware but is not necessary for termination hood measurements and will lead to signal distortions in the incomplete overlap range which can influence interpretation of these measurements.

We do agree that removing the overlap function can clarify the interpretation of the measurement. As a result, the figures have been updated to undo the overlap correction in the context of instrumental background signal. Another set of Figures S4 and S5 which include both range correction and overlap correction have been added to the supplement for better interpretation.

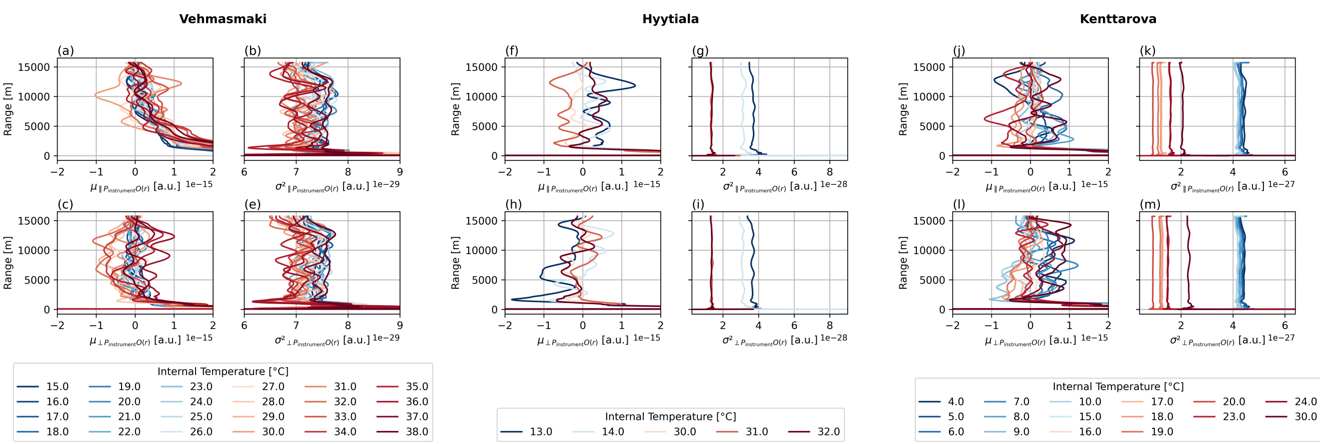

Figure 6. *Termination hood profiles at various internal temperatures (color-coded) across different sites. In Vehmasmaki: a) $\mu_{\parallel P_{\mathrm{instrument}} O(r)}$, b) $\sigma^2_{\parallel P_{\mathrm{instrument}} O(r)}$, c) $\mu_{\perp P_{\mathrm{instrument}} O(r)}$, and d) $\sigma^2_{\perp P_{\mathrm{instrument}} O(r)}$. In Hyytiala: f) $\mu_{\parallel P_{\mathrm{instrument}} O(r)}$, g) $\sigma^2_{\parallel P_{\mathrm{instrument}} O(r)}$, h) $\mu_{\perp P_{\mathrm{instrument}} O(r)}$, and i) $\sigma^2_{\perp P_{\mathrm{instrument}} O(r)}$. In Kenttärova: j) $\mu_{\parallel P_{\mathrm{instrument}} O(r)}$, k) $\sigma^2_{\parallel P_{\mathrm{instrument}} O(r)}$, l) $\mu_{\perp P_{\mathrm{instrument}} O(r)}$, and m) $\sigma^2_{\perp P_{\mathrm{instrument}} O(r)}$.*

Line 135: β_{mol}. is usually the molecular backscatter coefficient. What you rather should compare to find an aerosol-free region would be the hypothetical Rayleigh signal or β'_{mol}..

The details of the calculation could be provided already at this point and not in the next section.

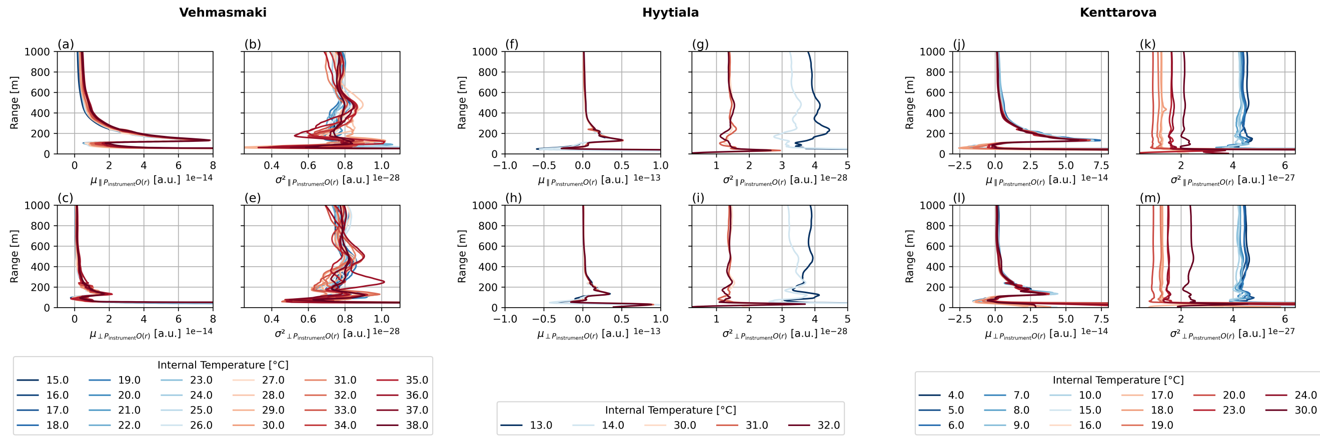

Figure 7. *Termination hood profiles at various internal temperatures (color-coded) across different sites only up to* $1000\ \mathrm{m}$ *range. In Vehmasmaki: a)* $\mu_{\parallel P_{\mathrm{instrument}}O(r)}$*, b)* $\sigma^2_{\parallel P_{\mathrm{instrument}}O(r)}$*, c)* $\mu_{\perp P_{\mathrm{instrument}}O(r)}$*, and d)* $\sigma^2_{\perp P_{\mathrm{instrument}}O(r)}$*. In Hyytiala: f)* $\mu_{\parallel P_{\mathrm{instrument}}O(r)}$*, g)* $\sigma^2_{\parallel P_{\mathrm{instrument}}O(r)}$*, h)* $\mu_{\perp P_{\mathrm{instrument}}O(r)}$*, and i)* $\sigma^2_{\perp P_{\mathrm{instrument}}O(r)}$*. In Kenttärova: j)* $\mu_{\parallel P_{\mathrm{instrument}}O(r)}$*, k)* $\sigma^2_{\parallel P_{\mathrm{instrument}}O(r)}$*, l)* $\mu_{\perp P_{\mathrm{instrument}}O(r)}$*, and m)* $\sigma^2_{\perp P_{\mathrm{instrument}}O(r)}$*.*

Thanks, this has been implemented.

Before the termination hood was applied, the μ_{ppol} *and* μ_{xpol} *profiles in the aerosol and hydrometeor-free region above* $5\ \mathrm{km}$ *closely follow the theoretical molecular attenuated backscatter coefficient* β'_{mol} *(Fig. 3b and c), indicating that the CL61 is sensitive to molecular scattering. The* β'_{mol} *profile was calculated following the method described by* **?** *using meteorological input data from a numerical weather prediction model available from the ACTRIS Cloudnet data portal...*

Line 147: See above. The overlap correction must be removed for the analysis. Perhaps the manufacturer can provide details if the correction is time dependent.

The instrument firmware applies a time-independent overlap correction to the measurements. It has now been removed from Figs. 6 and 7.

Line 148: Do you mean here "possible temperature dependence of the overlap function" instead of correction?

Thanks, this has been modified to explain that it is the instrumental background that has the temperature dependence.

It is likely that the observed bias is temperature-dependent and is caused by variations in instrumental background associated with afterpulsing, dark signal, and optical components under different temperature conditions

Line 149: Which temperature did you use? The CL61 measures `laser_temperature`, `internal_temperature`, and `transmitter_enclosure_temperature`.

`internal_temperature` was used. This clarification has been added to the text

To quantify the effect of temperature, the termination hood measurement was repeated over a range of internal temperatures T, reported as `internal_temperature` *in the instrument housekeeping data, across a two-year period.*

Line 153: Which diurnal pattern do you mean? Diurnal patterns are hardly visible in Fig. 3 (a) if only times from 11:00 until 16:00 are shown and only two hours are atmospheric measurements. In Fig. 1 (a) for instance, diurnal patterns are visible.

Thank you for spotting the mistake, it was meant to refer to Fig. 1.

The solar noise variance can be seen from the diurnal pattern in Fig. 1 and the difference between the σ^2 *profiles before (Fig. 3f and 3g) and during (Fig. 3h and 3i) the termination hood measurement.*

Line 162: Figure reference should be to Figure 3

Thank you for spotting the mistake, Fixed to refer to Fig. 3

Figure 3: The label in plot c) should be just β_{mol}..

Thank you for spotting the mistake, this is fixed

Line 168: Shouldn't a subscript "corrected" be added so that it isn't confused with Eq. 4?

Thanks, this has been implemented

$$ {}^{\parallel}\beta'_{\text{corrected}} = ppol - \mu_{{}^{\parallel}P_{\text{instrument}}(r,T)} r^2, \tag{3} $$

$$ {}^{\perp}\beta'_{\text{corrected}} = xpol - \mu_{{}^{\perp}P_{\text{instrument}}(r,T)} r^2, \tag{4} $$

Line 200: field of view should be added to Table 1

Thank you, this has been added

Receiver field-of-view $\pm\, 0.56\ \text{mrad}$

Line 215: What about the uncertainty in C which is not taken into account here? In line 224 you mention a 10% uncertainty. Did you average over several C values or have you applied a fit or trend with time between consecutive C values?

The C values were calculated on a monthly basis to ensure a sufficient number of data points for fitting within the theoretical range, while accounting for multiple scattering at different heights. Examples are provided in Figures S4 to S7 in the supplement.

To ensure robust data fitting, the cloud calibration is performed monthly using all suitable liquid cloud observations detected from the methodology.

Additionally, a revised equation incorporating a 10% uncertainty has been included.

The calibrated volume attenuated backscatter coefficient and its uncertainty can then be determined as follows, assuming the cloud calibration factor has an uncertainty of approximately 10% *(Hopkin et al., 2019):*

$$ \beta'_v = \beta'_{\text{corrected}} \cdot C, \tag{5} $$

$$ \sigma^2{}_{\beta'_v} = (\sigma^2{}_{\beta'_{\text{corrected}}} + 0.01 \cdot \beta'^2{}_{\text{corrected}}) \cdot C^2. \tag{6} $$

For those instruments where termination hood measurements are not available:

$$ \beta'_v = \beta' \cdot C, \tag{7} $$

$$ \sigma_{\beta'_v} = (\sigma^2{}_{P_{\text{atmosphere}}} + 0.01 \cdot \beta'^2) \cdot C^2 = (\sigma^2{}_{{}^{\parallel}P_{\text{atmosphere}}} + \sigma^2{}_{{}^{\perp}P_{\text{atmosphere}}} + 0.01 \cdot \beta'^2) \cdot C^2. \tag{8} $$

Line 217: Termination instead of terminal

Thank you for spotting the mistake, this is fixed.

For those instruments where termination hood measurements are not available:

Line 228: S_p instead of S

Thank you for spotting the mistake, this is fixed.

$$\sigma_{\beta_p}^2 = \left(\frac{\partial f}{\partial \beta_v'}\sigma_{\beta_v'}\right)^2 + \left(\frac{\partial f}{\partial C}\sigma_C\right)^2 + \left(\frac{\partial f}{\partial S}\sigma_{S_p}\right)^2. \quad (9)$$

Line 238: Termination instead of terminal

Thank you for spotting the mistake, this is fixed.

and δ_v *is the volume linear depolarization ratio, which is* $\delta_{\mathrm{corrected}}$ *in Eq. 17, or* $\frac{xpol}{ppol}$ *for instruments lacking termination hood measurements.*

Line 241: Which NWP model was used here?

ECMWF IFS forecast was used, This has been added to the text

The input data for these calculations are taken from a numerical weather prediction model (ECMWF IFS forecast) provided via the ACTRIS Cloudnet data portal...

Figure 6: Please align subplots vertically. Subplot e) should be d) to be consistent with the caption.

Thank you, this is fixed. See Fig. 6 and 7 in this reply.

Line 305: Can this conclusion be drawn on the basis of three measurements taken over a period of six months, even though the last value is actually in the middle?

This would be an important conclusion for operators. This plot should be shown not only in the supplements.

We will modify the wording of this statement and bring the Figure to the main manuscript.

Over a six-month period, the calibration profiles at each temperature show only minor fluctuations. Therefore, we recommend performing termination hood checks at least once across the operating temperature range to determine the instrumental background signal bias and noise.

Section 4.4: Is a single profile shown or is an average over a time period discussed? What would be the influence on the uncertainty if averaged over several profiles? It would be nice to see profiles compared.

It shows a single profile. If multiple profiles were averaged, the uncertainty would be reduced by approximately a factor of $\sqrt{n}$, where n is the number of profiles, assuming each profile has similar uncertainty. Clarification regarding the figure is added, as well as an extra figure in the supplement showing the effect of averaging multiple profiles in 10 minutes.

Figure 10 presents the β, δ *and their associated uncertainties in the aerosol layer below* $1000\ \mathrm{m}$ *obtained from a measurement profile recorded at 13:00 UTC on the same day.*

Averaging multiple profiles reduces the uncertainties, as illustrated in Fig. S13, which shows the profiles averaged over 10 minutes.

To give a better idea, one could also mention some typical values for the depolarization ratio.

The following has been added:

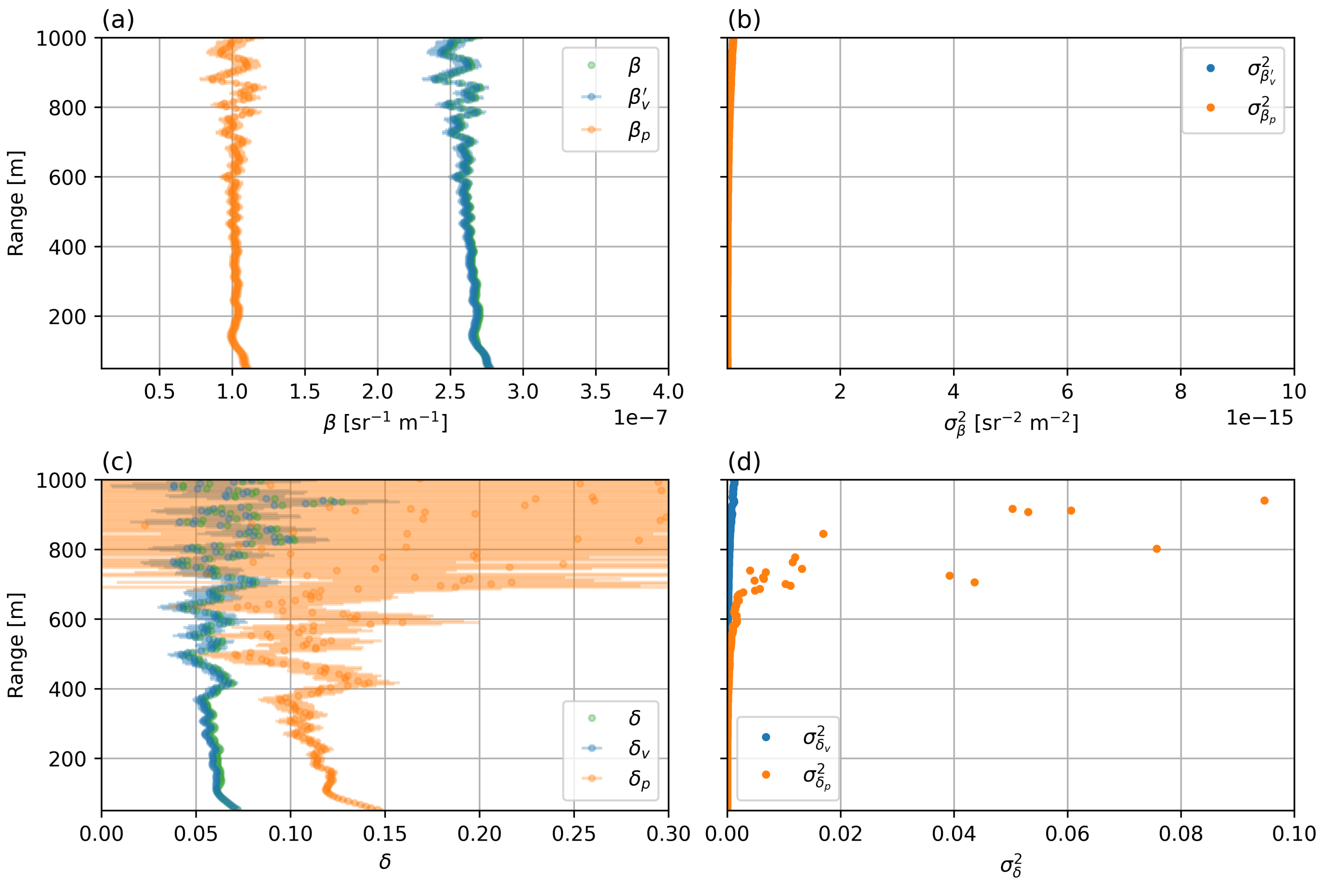

Figure S13. *Example of uncorrected and corrected profiles in Kenttärova, averaged from 2024-06-04 13:00 to 13:10 UTC. a) β, β'_v, β_p, b) $\sigma^2_{\beta'_v}$, $\sigma^2_{\beta_p}$, c) δ, δ_v, δ_p, d) $\sigma^2_{\delta_v}$, $\sigma^2_{\delta_p}$.*

During pollen seasons in Finland, δ_p has been observed at 0.23 ± 0.06 for pine and 0.26 ± 0.06 for birch at this wavelength (Filioglou et al., 2023).

The authors might also consider plotting the various parameters as line plots, with the margin of uncertainty shown as a shaded area or error bars.

Thank you, this has been implemented

Line 349: Termination hood measurement

Thanks, it has been fixed

....the termination hood remains important as it allows the estimation of measurement uncertainty.

Figure 10: Why was for the subplots e)-h) another y-axis range chosen?

Because this is the result of the aerosol particle inversion, which focuses on the aerosol measurement. This has been added to the figure caption:

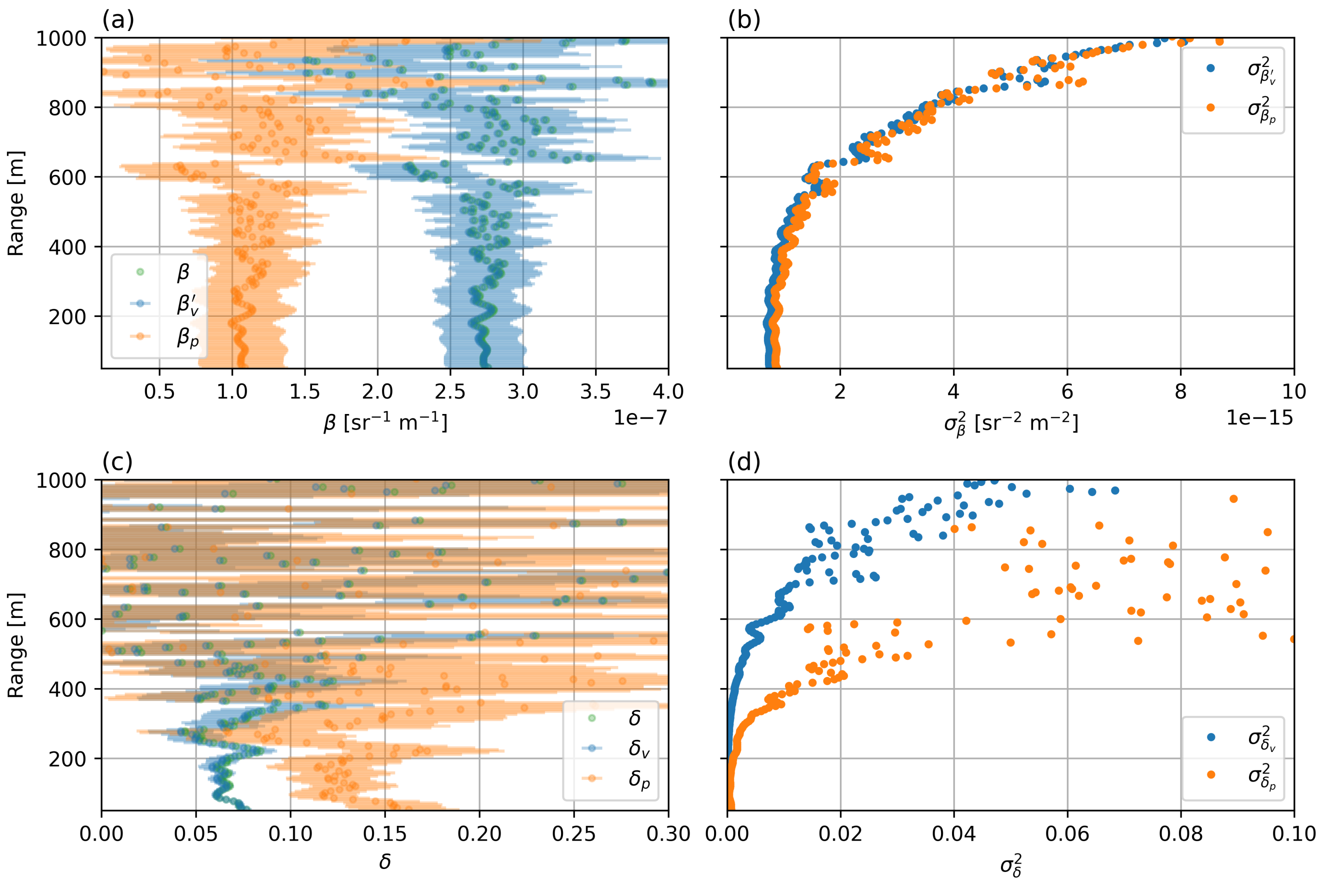

Figure 10. *Example of uncorrected and corrected profiles in Kenttarova measured at 2024-06-04 13:01 UTC. a) β, β'_v, β_p, b) $\sigma^2_{\beta'_v}$, $\sigma^2_{\beta_p}$, c) δ, δ_v, δ_p, d) $\sigma^2_{\delta_v}$, $\sigma^2_{\delta_p}$.*

For particle properties in panels e-h, profiles are shown only up to 1 km *range.*

Section 4.5: What was the reason for the high humidity inside the instrument? Was there a sealing problem with the window? Adding the relative humidity from the housekeeping data to the plot would help operators to see above which values this problem can happen.

We do not know the exact cause; it may be related to the window seal, although the problem persists even after its replacement. The relative humidity has been added to the Figure 12. However, the main issues here is that the condensation happens only at the window that is exposed to outside temperature while the relative humidity inside the instrument is still low. It can be thought of as a cold soda can in a room temperature. Condensation occurs at cold surface despite low relative humidity. We updated figure with internal relative humidity measurement and added a paragraph to the manuscript.

This occurred despite the measured internal relative humidity remaining below 70%. This is because the measurement does not represent the relative humidity at the window surface, where temperature is closer to ambient temperature.

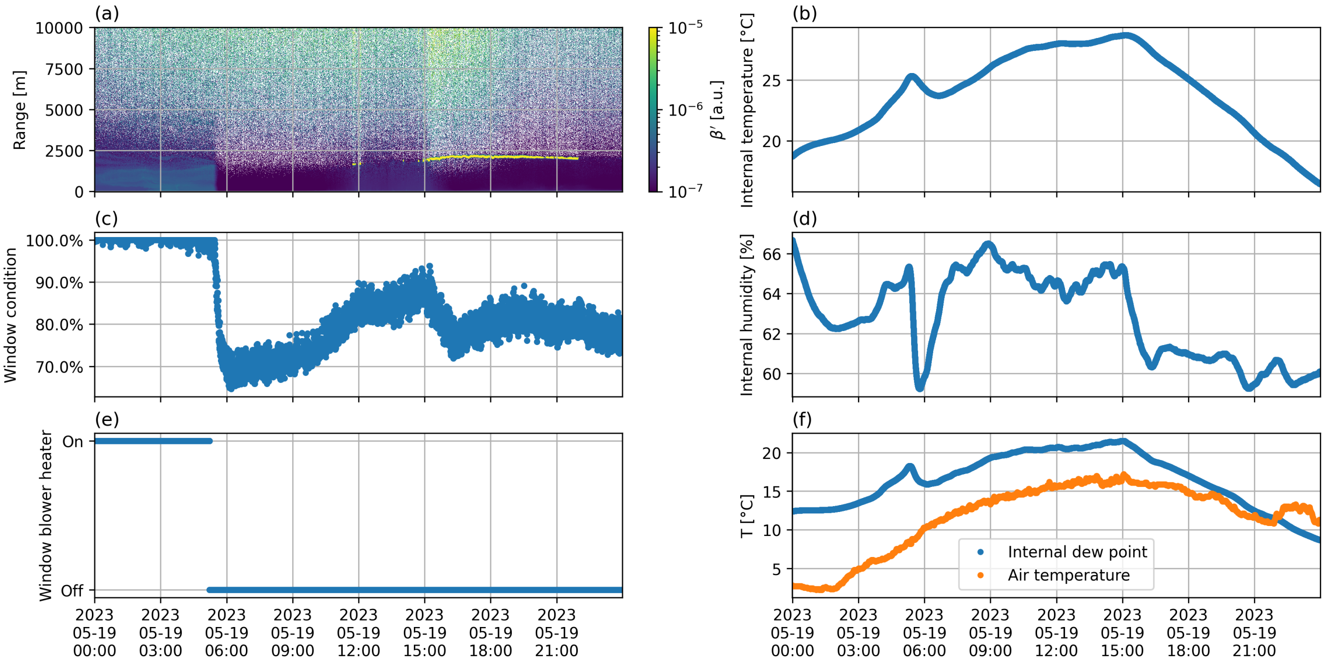

Figure 12. *Measurements from Vehmasmäki on 2023-05-19 a) β', b) Internal temperature, c) window condition, d) Internal humidity, e) Window blower heater, f) Calculated dew point and measured outside air temperature*

Line 379: A temperature dependence of the overlap function was not clearly visible in Figure 7. Can this be stated here?

As also noted by referee 1, we modified it to be the temperature dependence of the instrumental background bias and noise. This temperature dependence is shown in Fig. 6 and Fig. 7, and even more clearly in Fig. S4 and Fig. S5 below 1 km without the range and overlap correction.

Termination hood measurements were performed on selected instruments and proved effective in characterizing the instrumental background bias and noise profiles and and their temperature dependence.

Line 384: See comment for line 305. The results in Figure S3 do not really support that conclusion here.

We have reconsidered the recommendation, and have reformulated it as follows:

Over a six-month period, the calibration profiles at each temperature show only minor fluctuations. Therefore, we recommend performing termination hood checks at least once across the operating temperature range to determine the instrumental background signal bias and noise.

Line 392: If quantitatively analyzing aerosol optical properties with lidar at this wavelength and at even longer wavelength, the molecular contribution must always taken into account. The difference in the backscatter coefficient is approximately the molecular backscatter coefficient at around 910 nm at ground level which can be calculated. Also the difference in is strongly dependent on the aerosol type and load and on altitude. It is not possible to make a general statement about the difference here, but it is clear that the molecular component must be taken into account.

We revised the text to emphasize the contribution of this study in presenting an approach for estimating measurement uncertainties using termination hood measurements. We also removed the general statement and made the conclusion regarding difference in depolarization ratio more specific to the low-aerosol conditions typically encountered in Finland.

Nevertheless, the termination hood measurements remain crucial, as they allow the instrumental background to be quantified and subsequently used to estimate the uncertainties of β_p *and* δ_p*, as presented in this study. For typical low aerosol load conditions in Finland, as in this study case, we found that the difference between* β_p *and* β *is approximately* $1.5\times10^{-7}\ \mathrm{sr}^{-1}\ \mathrm{m}^{-1}$*, and that between* δ *and* δ_p *is roughly* 0.1 *in the near surface layer.*

Line 395: Is it the fogging of the optical lens or the window?

It's the window, thanks for spotting the mistake

Additionally, some instruments experienced signal loss caused by the fogging of the window, which resulted in degraded data quality.

References

Filioglou, M., Leskinen, A., Vakkari, V., O'Connor, E., Tuononen, M., Tuominen, P., Laukkanen, S., Toiviainen, L., Saarto, A., Shang, X., Tiitta, P., and Komppula, M.: Spectral dependence of birch and pine pollen optical properties using a synergy of lidar instruments, Atmospheric Chemistry and Physics, 23, 9009–9021, https://doi.org/10.5194/acp-23-9009-2023, 2023.

Hopkin, E., Illingworth, A. J., Charlton-Perez, C., Westbrook, C. D., and Ballard, S.: A robust automated technique for operational calibration of ceilometers using the integrated backscatter from totally attenuating liquid clouds, Atmospheric Measurement Techniques, 12, 4131–4147, https://doi.org/10.5194/amt-12-4131-2019, 2019.